

A LEVEL-SET METHOD FOR INTERFACIAL HEAT OR MASS TRANSFER IN TWO-PHASE FLOWS

NÉSTOR BALCÁZAR^{2,1}, OSCAR ANTEPARA¹, JOAQUIM RIGOLA¹
AND ASSENSI OLIVA¹

¹ Heat and Mass Transfer Technological Center (CTTC), Universitat Politècnica de Catalunya
- BarcelonaTech (UPC)
ETSEIAT, Colom 11, 08222 Terrassa (Barcelona), Spain.
web page: <http://www.cttc.upc.edu/>

² Termo Fluids S.L.
Avda Jacquard 97 1-E, 08222 Terrassa (Barcelona), Spain
e-mail: nestor@cttc.upc.edu, web page: <http://www.termofluids.com/>

Key words: Conservative level-set, Two-phase flow, Bubbles and Droplets, Interfacial mass transfer, Interfacial heat transfer

Abstract. A level-set model is proposed for simulating interfacial heat or mass transfer in two-phase flows. The Navier-Stokes equations as well as the heat transfer or mass transfer equations are discretized using a finite-volume approach on a collocated unstructured mesh, whereas a multiple marker level-set methodology is introduced in order to avoid the numerical coalescence of the fluid interfaces. Some numerical examples are considered to show the capabilities of this model, including pure diffusion of a chemical species with chemical reaction, and buoyancy-driven motion of bubble swarms with mass transfer. Present results are compared against analytical and empirical correlations from the literature as validations of the proposed model.

1 INTRODUCTION

Bubbly flows with heat transfer or mass transfer are common in natural phenomena and technological applications [26]. Some applications can be found in the so-called unit operations of the chemical engineering, where bubble columns are used as chemical and biochemical reactors. Although some empirical correlations have been proposed for estimation of heat and mass transfer coefficients in bubbles or droplets [17], there is a lack of understanding of the interplay between fluid mechanics and interfacial mass transfer (or heat transfer). Since these small-scale phenomena affect the overall operation and control of multiphase systems, as well for future optimization and design, it is of great importance to improve the accuracy of these models.

The physical description of bubbly flows with heat transfer and mass transfer, lead to a complex and highly non-linear mathematical problem. Indeed, theoretical methods can be used to the simplest cases, whereas experimental measurements can be difficult due to

limitations in optical access. On the other hand, the combination of High Performance Computing (HPC) and Direct Numerical Simulation (DNS) of the Navier-Stokes equations open the possibility to design non-invasive and controlled experiments of bubbly flows, enabling an accurate control of the bubble size distribution, deformability, coalescence, and flow conditions. In this sense, multiple methods have been introduced in the last decades for DNS of two-phase flows, for instance: volume-of-fluid (VOF) methods [23], level-set (LS) methods [28, 32, 27, 4], coupled VOF/LS methods [7], and front tracking (FT) methods [34]. Furthermore, some numerical models have been proposed for heat transfer or mass transfer at deformable fluid interfaces [20, 13, 14, 2, 35, 15, 19]. However, DNS of heat transfer or mass transfer in bubble swarms are still quite limited, and only few works have been published [21, 1, 30, 24]. Although previous papers touched upon heat or mass transfer in single bubbles or droplets using VOF, LS and FT methods, to the best of the authors' knowledge, there are no previous studies in the context of the conservative level-set (CLS) method [27, 4]. Indeed, this work aims to present a novel numerical methodology for simulating interfacial heat transfer or mass transfer in bubbly flows, which extends a multiple marker CLS approach introduced in our previous works [5, 8]. This approach includes the adoption of three-dimensional collocated unstructured meshes [4], as well as adaptive mesh refinement for hexahedral meshes [3]. Since a CLS method [4] is used, accumulation of mass conservation error is circumvented, whereas the multiple marker methodology [5, 8] avoids the numerical and potentially unphysical merging of the fluid interfaces, taken into account the physics of bubble collisions in long-time simulations of bubbly flows.

This paper is organized as follows: The mathematical formulation and numerical methods are presented in section 2. Numerical experiments are presented in section 3. Finally, concluding remarks and future work are discussed in section 4.

2 MATHEMATICAL FORMULATION AND NUMERICAL METHODS

2.1 Incompressible two-phase flow

The Navier-Stokes equations for the dispersed fluid (Ω_d) and continuous fluid (Ω_c) can be combined into a set of equations in a global domain $\Omega = \Omega_d \cup \Omega_c$, with a singular source term for the surface tension force at the interface Γ [34, 4]:

$$\frac{\partial}{\partial t}(\rho \mathbf{v}) + \nabla \cdot (\rho \mathbf{v} \mathbf{v}) = -\nabla p + \nabla \cdot \mu (\nabla \mathbf{v} + (\nabla \mathbf{v})^T) + (\rho - \rho_0) \mathbf{g} + \mathbf{f}_\sigma \delta_\Gamma, \quad (1)$$

$$\nabla \cdot \mathbf{v} = 0, \quad (2)$$

where \mathbf{v} is the fluid velocity, p denotes the pressure field, ρ is the fluid density, μ is the dynamic viscosity, \mathbf{g} is the gravitational acceleration, $\mathbf{f}_\sigma \delta_\Gamma$ is the surface tension force, δ_Γ is the Dirac delta function concentrated at the interface, subscripts d and c denote the dispersed phase and continuous phase respectively. Physical properties are constant at each fluid-phase with a jump discontinuity at the interface:

$$\rho = \rho_d H_d + \rho_c (1 - H_d), \quad \mu = \mu_d H_d + \mu_c (1 - H_d), \quad (3)$$

where H_d is the Heaviside step function that is one at fluid d and zero elsewhere. At discretized level a continuous treatment of physical properties is adopted in order to avoid numerical instabilities at the interface [4]. If periodic boundary condition is applied on the $y - axis$ (aligned to \mathbf{g}), then a force $-\rho_0\mathbf{g}$ is added to the Navier-Stokes equations (Eq. (1)), with $\rho_0 = V_\Omega^{-1} \int_\Omega (\rho_d H_d + \rho_c(1 - H_d)) dV$, to prevent the acceleration of the entire flow field in the downward vertical direction due to the action of \mathbf{g} [31, 5, 9]. On the other hand, $\rho_0 = 0$ for simulations without periodic boundary conditions on the $y - axis$.

2.2 Multiple marker level-set method

The conservative level-set method (CLS) introduced by [4] for interface capturing on unstructured grids is used in this work. Furthermore, in order to avoid the numerical coalescence of the fluid interfaces, each fluid particle is represented by a CLS function, according to the multiple marker CLS method introduced by [5, 8, 9]. In this method, the interface of the i th fluid particle is defined as the 0.5 iso-surface of a regularized indicator function ϕ_i , where $i = 1, 2, \dots, n_d$ and n_d is the total number of fluid particles in the dispersed phase. Since the velocity field is solenoidal (Eq. 2), the i th interface transport equation can be written in conservative form:

$$\frac{\partial \phi_i}{\partial t} + \nabla \cdot \phi_i \mathbf{v} = 0, \quad i = 1, 2, \dots, n_d. \quad (4)$$

Furthermore, an additional re-initialization equation is introduced in order to keep a sharp and constant interface profile:

$$\frac{\partial \phi_i}{\partial \tau} + \nabla \cdot \phi_i (1 - \phi_i) \mathbf{n}_i = \nabla \cdot \varepsilon \nabla \phi_i, \quad i = 1, 2, \dots, n_d. \quad (5)$$

This equation is advanced in pseudo-time τ up to steady state. It consists of a compressive term, $\phi_i(1 - \phi_i)\mathbf{n}_i|_{\tau=0}$, which forces the level-set function to be compressed onto the interface along the normal vector \mathbf{n}_i , and of a diffusion term, $\nabla \cdot \varepsilon \nabla \phi_i$, to maintain the CLS profiles with characteristic thickness $\varepsilon = 0.5h^{0.9}$, where h is the grid size [4, 8].

Geometrical information on the interface Γ_i , such as normal vectors \mathbf{n}_i and curvatures κ_i are obtained as follows:

$$\mathbf{n}_i(\phi_i) = \frac{\nabla \phi_i}{\|\nabla \phi_i\|}, \quad \kappa_i(\phi_i) = -\nabla \cdot \mathbf{n}_i. \quad (6)$$

Surface tension forces are calculated by the continuous surface force model [16], extended to the multiple marker CLS method in our previous work [5, 8, 9]:

$$\mathbf{f}_\sigma \delta_\Gamma = \sum_{i=1}^{n_d} \sigma \kappa_i(\phi_i) \nabla \phi_i. \quad (7)$$

Finally, in order to avoid numerical instabilities at the interface, fluid properties in Eq. 3 are regularized by means of a global level-set function $H_d = \phi_d$ [5, 8] defined as:

$$\phi_d(\mathbf{x}, t) = \max\{\phi_1(\mathbf{x}, t), \dots, \phi_{n_d-1}(\mathbf{x}, t), \phi_{n_d}(\mathbf{x}, t)\}. \quad (8)$$

2.3 Mass transfer

In this research, it is assumed that convection, diffusion and reaction of the mass dissolved from the dispersed phase Ω_d exists only in the continuous phase Ω_c , whereas the concentration inside the bubbles is kept constant [19, 30, 1]. This assumption is valid for moderately soluble substances [17], moreover, bubbles do not shrink and the concentration is not coupled to the hydrodynamics. Therefore, the mass transfer of a chemical species is given by the following convection-diffusion-reaction equation, which is only considered in the continuous phase Ω_c :

$$\frac{\partial C}{\partial t} + \nabla \cdot (\mathbf{v}C) = \nabla \cdot (\mathcal{D}\nabla C) + \dot{r}, \quad (9)$$

where C is the concentration of the dissolved species, \mathcal{D} is the diffusion coefficient which takes the value \mathcal{D}_c in Ω_c and \mathcal{D}_d in Ω_d , \dot{r}_j denotes the overall chemical reaction rate, e.g. $\dot{r}_j = -k_1 C$ with k_1 defined as the first-order reaction rate constant.

Given a cell Ω_P and its neighbor cells Ω_i with common vertexes, and the global level-set function ϕ_d defined in Eq. (8), then Ω_P is an interface cell if there is at least one cell Ω_i for which $\phi_{d,P} > 0.5$ and $\phi_{d,i} < 0.5$, or $\phi_{d,P} < 0.5$ and $\phi_{d,i} > 0.5$, or if $\phi_{d,P} = 0.5$. Here the subindex P denotes the current cell, and subindex i denotes the neighbor cell. In this context, the concentration of the dissolved species (C) at the interface cells is computed by linear interpolation, using information of the concentration field from the continuous fluid phase Ω_c (excluding interface cells). This linear interpolation is performed using a nodes stencil $\{P, I, F_p\}$, P denotes the node at the current interface cell Ω_P , I denotes a point at the interface, F_p denotes the projection of the node F on the line l_p , F is the closest node to the line l_p selected from the neighbor nodes of P , in a region of two cell layers around Ω_P , l_p is a line orthogonal to the interface which contains the points \mathbf{x}_P and \mathbf{x}_I . Indeed, C_P is computed as follows:

$$C_P = C_I - \frac{\|\mathbf{x}_I - \mathbf{x}_P\|}{\|\mathbf{x}_I - \mathbf{x}_{F_p}\|} (C_I - C_{F_p}), \quad (10)$$

where $C_{F_p} = C_F + (\mathbf{x}_{F_p} - \mathbf{x}_F) \cdot (\nabla_h C)_F$. The minimum distance from the point F_p to the interface Γ is approximated as follows: $\|\mathbf{x}_I - \mathbf{x}_{F_p}\| = \|\mathbf{x}_I - \mathbf{x}_P\| + |\mathbf{n}_P \cdot (\mathbf{x}_F - \mathbf{x}_P)|$, with $\mathbf{n}_P = (\nabla_h \phi_d)_P / \|(\nabla_h \phi_d)_P\|$. The distance function at the cell P , $|d(\mathbf{x}_P, t)|$, is calculated from the CLS function $\phi_d(\mathbf{x}_P, t)$, as follows: $\|\mathbf{x}_I - \mathbf{x}_P\| = |2\varepsilon (\tanh^{-1}(2\phi_d(\mathbf{x}_P, t)) - 1)|$ [4, 27].

2.4 Numerical methods

The Navier-Stokes equations, Eq. (1-2), interface capturing equations, Eqs. (4-5), and mass transfer equation, Eq. (9), are solved with a finite-volume discretization of the physical domain on a collocated unstructured mesh [4], where both scalar and vector variables (p , \mathbf{v} , ϕ , ρ and μ) are stored in the cell centroids. Following [4], the convective term of momentum equation (Eq. (1)), interface transport equation (Eq. (4)), and mass transfer equation (Eq. (9)), is explicitly computed approximating the fluxes at cell faces

with a Total Variation Diminishing (TVD) Superbee limiter scheme [4]. Diffusive terms are centrally differenced, whereas a distance-weighted linear interpolation is used to find the cell face values of physical properties and interface normals, unless otherwise stated. Gradients are computed at cell centroids by means of the least-squares method [4]. A central difference scheme is used to discretize both compressive and diffusive terms of the re-initialization equation (Eq. (5)). The resolution of the velocity and pressure fields is achieved using a standard fractional-step projection method originally developed by [18]. In the first step a predictor velocity (\mathbf{v}^*) is computed as follows:

$$\frac{\rho \mathbf{v}^* - \rho^n \mathbf{v}^n}{\Delta t} = \mathbf{C}_v^n + \mathbf{D}_v^n + (\rho - \rho_0) \mathbf{g} + \sum_{i=1}^{n_d} \sigma \kappa_i(\phi_i) \nabla_h \phi_i, \quad (11)$$

where super-index n denotes the previous time step, $\mathbf{D}_v(\mathbf{v}) = \nabla_h \cdot \mu \nabla_h \mathbf{v} + \nabla_h \cdot \mu (\nabla_h \mathbf{v})^T$, $\nabla_h \cdot \mu \nabla_h \mathbf{v}$ is approximated by a central difference scheme, $\nabla_h \cdot \mu (\nabla_h \mathbf{v})^T$ is calculated by the Gauss-Theorem [4], $\nabla_h \phi_i$ and $(\nabla_h \mathbf{v})^T$ are evaluated by using the least-squares method [4], $\kappa_i(\phi_i)$ is obtained at each cell according to Eq. (6), and $\mathbf{C}_v(\rho \mathbf{v}) = -\nabla_h \cdot (\rho \mathbf{v} \mathbf{v})$ is discretized using flux limiters schemes [4, 8]. In a second step a corrected velocity (\mathbf{v}) is computed by:

$$\frac{\rho \mathbf{v} - \rho \mathbf{v}^*}{\Delta t} = -\nabla_h(p), \quad (12)$$

Furthermore, imposing $\nabla_h \cdot \mathbf{v} = 0$ to Eq. (12) results in a Poisson equation for the pressure field, which is solved by means of a preconditioned conjugate gradient method:

$$\nabla_h \cdot \left(\frac{1}{\rho} \nabla_h p \right) = \frac{1}{\Delta t} \nabla_h \cdot (\mathbf{v}^*), \quad \mathbf{e}_{\partial\Omega} \cdot \nabla_h p|_{\partial\Omega} = 0. \quad (13)$$

Finally, a cell-face velocity \mathbf{v}_f [4, 8] is used to advect momentum (Eq. (1)), CLS functions (Eq. (4)), and concentration (Eq. (9)). This velocity is defined to fulfill the incompressibility constraint in each control volume, Eq. 2, and to avoid pressure-velocity decoupling when the pressure projection is made on collocated meshes [29]:

$$\mathbf{v}_f = \sum_{q \in \{P, F\}} w_q \left(\mathbf{v}_q + \frac{\Delta t}{\rho_q} (\nabla_h p)_q \right) - \frac{\Delta t}{\rho_f} (\nabla_h p)_f, \quad (14)$$

where P and F are the control volumes with common face f [4, 8], $w_q = 0.5$, ρ_f is calculated by arithmetic averaging. The reader is referred to Appendix B of our previous work [8] for further technical details on the origin of Eq. (14).

A TVD Runge-Kutta method [22] is used for time integration of advection equation (Eq. (4)) and re-initialization equation (Eq. (5)). Solving Eq. (5) up to steady-state results in a smooth transition of ϕ_i at the interface, proportional to the diffusion coefficient $\varepsilon = 0.5h^{0.9}$, where h is the grid size [4]. One iteration per physical time step of the re-initialization Eq. (5) is sufficient to keep the profile of the CLS functions in present work [4, 7].

Present numerical algorithms are implemented in the framework of an in-house parallel C++/MPI code called TermoFluids [33]. The code is run on the supercomputer MareNostrum IV using a range of 96 – 576 CPU cores for 3D simulations of bubbly flows. The reader is referred to [4, 5, 6, 8, 9] for additional technical details on the finite-volume discretization of Navier-Stokes equations, energy equation and level-set equations on collocated unstructured grids.

3 NUMERICAL EXPERIMENTS

Validations and verifications of the CLS method [4] have been reported in our previous works, for instance: dam-break problem and gravity-driven motion of single bubbles [4, 6], binary droplet collision with bouncing outcome [5], drop collision against a fluid interface without coalescence [5], bubbly flows in vertical channels [9, 11], falling droplets [10], Taylor bubbles [12], and thermocapillary-driven motion of deformable droplets [7]. Therefore, this research can be considered a further step in the development of numerical methods for simulation of bubbly flows with interfacial mass transfer (or heat transfer) using unstructured meshes.

Regarding validation and verification of this numerical model, present numerical experiments are focused on DNS of gravity-driven bubbly flows with mass transfer. Therefore, the relevant physical quantities are summarized as follows: $\sigma, g, U_T, d, \rho_d, \rho_c, \mu_d, \mu_c$, where U_T is the rise velocity and $d = (6V/\pi)^{1/3}$ is the initial spherical volume equivalent diameter of the bubble. Nondimensionalization results in next parameters [17]:

$$Mo \equiv \frac{g\mu_c^4\Delta\rho}{\rho_c^2\sigma^3}, \quad Eo \equiv \frac{gd^2\Delta\rho}{\sigma}, \quad Re \equiv \frac{\rho_c U_T d}{\mu_c}, \quad \eta_\rho \equiv \frac{\rho_c}{\rho_d}, \quad \eta_\mu \equiv \frac{\mu_c}{\mu_d}, \quad (15)$$

where, η_ρ is the density ratio, η_μ is the viscosity ratio, Mo is the Morton number, $\Delta\rho = |\rho_c - \rho_d|$ is the density difference between the fluid phases, subscript d denotes the dispersed fluid phase, subscript c denotes the continuous fluid phase, Eo is the Eötvös number, Re is the Reynolds number, and $t^* = t\sqrt{g/d}$ is the dimensionless time. Moreover, numerical results for each bubble ($Re_i(t)$) will be reported in terms of the so-called drift velocity [31], $(U_T)_i(t) = (\langle \mathbf{v}_i \rangle(t) - \langle \mathbf{v}_c \rangle(t)) \cdot \mathbf{e}_y$, defined as the bubble velocity with respect to a stationary container, where $\langle \mathbf{v}_i \rangle(t)$ is the velocity of the bubble centroid, $\langle \mathbf{v}_c \rangle(t)$ is the spatial averaged velocity of the continuous fluid in Ω_c .

In addition, large-scale models incorporates closures for mass transfer by means of a Sherwood correlation, $Sh = f(Re, Sc)$, whereas it is expected an effect of the bubble fraction α in bubble swarms. Mass transfer in bubbly flows can be characterized by the Sherwood number (Sh) and, Schmidt number (Sc) or Peclet number (Pe), defined in Ω_c as follows:

$$Sh = \frac{k_L d}{\mathcal{D}_c}, \quad Sc = \frac{\mu_c}{\rho_c \mathcal{D}_c}, \quad Pe = \frac{U_T d}{\mathcal{D}_c} = Re Sc, \quad (16)$$

with k_L defined as the liquid-side mass transfer coefficient. Simulation of bubbly flows with mass transfer is performed in a fully periodic domain (Section 3.2). Therefore, saturation of chemical species concentration is avoided by including a first order chemical

reaction in Ω_c [30]. The mass transfer coefficient ($k_L(t)$) in bubbly flow with mass transfer and first order chemical reaction (Section 3.2) is computed as follows:

$$k_L(t) = \frac{V_{\Omega_c} k_1 \langle C \rangle_{\Omega_c}(t)}{(HC_0 - \langle C \rangle_{\Omega_c}(t)) \sum_{i=1}^{nd} A_i(t)} \quad (17)$$

where V_{Ω_c} is the volume of Ω_c , H is the Henry constant ($H = 1$ unless otherwise stated), C_0 is the concentration inside the bubble, $A_i(t) = \int_{\Omega} \|\nabla \phi_i\| dV$ is the bubble surface, $\langle C \rangle_{\Omega_c}(t)$ is the spatial averaged concentration in Ω_c .

3.1 Diffusion of a stationary spherical bubble

The validation of the numerical model to solve the mass transfer equation (Eq. (9)) is performed by comparing simulation result of stationary spherical bubble in a quiescent liquid pool with analytical solution. At steady state, the mass transfer of a chemical species with first order chemical reaction, in spherical coordinates is written as:

$$\frac{\mathcal{D}_c}{r^2} \frac{\partial}{\partial r} \left(r^2 \frac{\partial C}{\partial r} \right) - k_1 C = 0 \quad (18)$$

which has the following analytical solution:

$$C(r) = C_0 \frac{d}{2r} \frac{e^{-ar}}{e^{-ad/2}} \quad (19)$$

with $a = (k_1/\mathcal{D}_c)^{1/2}$, C_0 is the concentration inside the bubble and d is the bubble diameter.

In this simulation, the bubble of diameter d , is fixed at the center of a cubic domain $\Omega = [0, 3.6d] \times [0, 3.6d] \times [0, 3.6d]$. Furthermore $k_1 = 0.5$, $\mathcal{D}_c = 5 \times 10^{-4}$, $C_0 = 1$ and $d = 0.277$. The velocity field is set to $\mathbf{v} = \mathbf{0}$ in the whole domain, whereas the initial concentration is one inside the droplet and zero otherwise. Neumann boundary condition is used on the confining boundary. The mesh is conformed by uniform and tetrahedral control volumes, with averaged grid sizes $h = \{d/36, d/18, d/9\}$ and number of control volumes $N_{cv} = \{29.5M, 3.6M, 0.5M\}$ respectively. Comparison between the continuous radial concentration profile and the analytical solution is presented in Fig. 1-a for different grid sizes (h). As can be seen there is a close agreement between the computed concentration and the exact solution, moreover the accuracy increases with grid refinement. Fig. 1-b shows species concentration field at steady state. It is observed that the species diffuses from the bubble to the continuous liquid phase, as a consequence of the concentration gradient at the interface. Therefore this validation indicates that the present method has been correctly implemented on unstructured meshes.

3.2 Mass transfer in bubble swarms

Ω is defined as a cube of length-side $4d$, where d is the initial bubble diameter. Ω is divided in $8M$ uniform hexahedral cells, with grid size $h = d/50$, distributed on 576

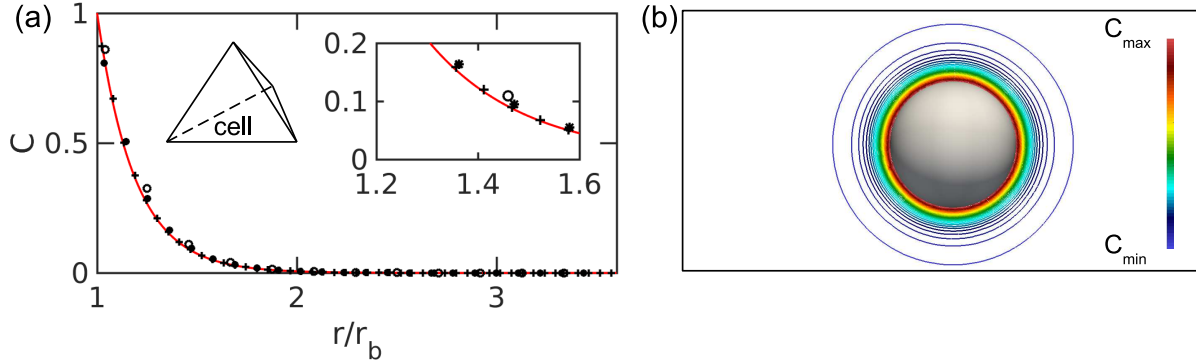


Figure 1: Mass transfer with first order chemical reaction from a stationary spherical bubble, at steady state. (a) Grid convergence, mesh conformed by tetrahedral cells, grid size $h = d/36$ (+), $h = d/18$ (*) and $h = d/9$ (o). Analytical solution (continuous red line). (b) Concentration field at steady state, $h = d/36$.

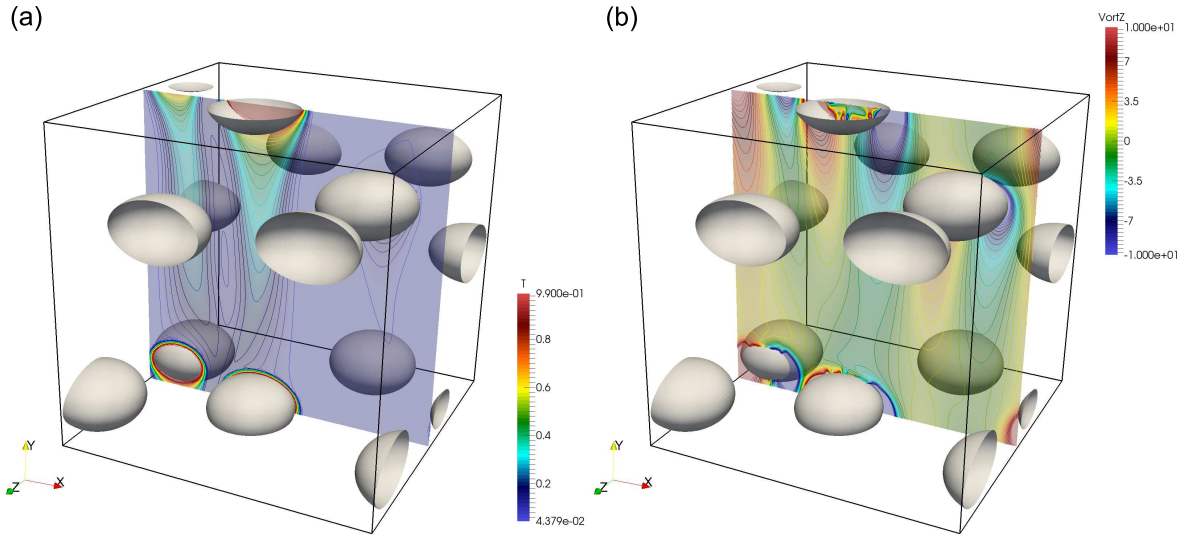


Figure 2: Mass transfer with first order chemical reaction from a bubble swarm (8 bubbles) in a cubic periodic domain, at $t^* = tg^{1/2}d^{-1/2} = 62.6$. $EO = 3.125$, $Mo = 5 \times 10^{-6}$, $\eta_\rho = \eta_\mu = 100$, $Sc = 10$, $\alpha = 6.5\%$. (a) Concentration contours on a plane $x - y$. (b) Vorticity contours, $\Omega_z = \mathbf{e}_z \cdot \nabla \times \mathbf{v}$, on a plane $x - y$.

processors. Periodic boundary conditions are used on the $x - y$, $y - z$ and $x - z$ boundary planes. At the beginning, bubbles are initially placed in Ω following a random pattern, whereas the fluid phases are quiescent. Since fluids are assumed to be incompressible and bubble merging is not allowed, the void fraction ($\alpha = V_{bubbles}/V_\Omega$) and the number of bubbles are constant throughout the simulation.

Dimensionless parameters used in this simulation are $EO = 3.125$, $M = 5 \times 10^{-6}$, $\eta_\rho = 100$, $\eta_\mu = 100$, $Sc = 10$, $\alpha = 6.5\%$, and $k_1 d^2 \mathcal{D}_c^{-1} = 79.7$. corresponding to dilute bubbly flows with 8 bubbles contained in the periodic cube. Fig. 2 shows an snapshot of the motion of a swarm of 8 bubbles in a full periodic domain at $t^* = 65.6$, and slices

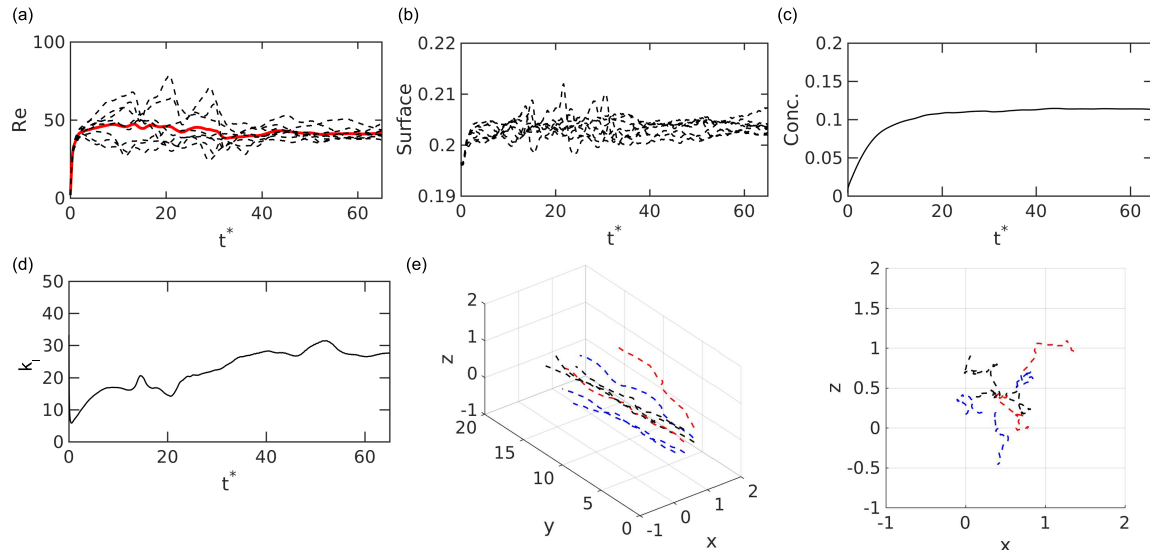


Figure 3: Mass transfer with first order chemical reaction from a bubble swarm (8 bubbles) in a cubic periodic domain. $Eo = 3.125$, $Mo = 5 \times 10^{-6}$, $\eta_\rho = \eta_\mu = 100$, $Sc = 10$, $\alpha = 6.5\%$. Time evolution for: (a) Reynolds number for each bubble, and average Reynolds number (red line). (b) Bubble surface. (c) Chemical species averaged concentration in Ω_c . (d) Mass transfer coefficient (k_l). (e) Bubble trajectories.

of concentration field C (Fig. 2a) and vorticity field $\mathbf{e}_y \cdot \nabla \times \mathbf{v}$ (Fig. 2b) on the plane $x - y$. Fig. 3 depicts the time evolution of Reynolds number $Re_i(t)$, bubble surface $A_i(t)$, chemical species concentration averaged in Ω_c , mass transfer coefficient $k_L(t)$ computed by means of Eq. (17), and bubble trajectories. Furthermore, Fig. 3a illustrates that $Re_i(t)$ presents an oscillatory and transient behaviour due to the bubble-bubble interactions according to the so-called drafting-kissing-tumbling phenomenon [5, 9, 10], whereas the bubble swarm achieves a quasi-steady steady state after $t^* \sim 40$. Regarding the chemical species averaged concentration in Ω_c (Fig. 3c) and mass transfer coefficient (Fig. 3d), these tend also to a quasi steady-state at $t^* \sim 40$.

4 CONCLUSIONS

A level-set model for interfacial mass transfer (or heat transfer) in two-phase flows has been introduced. From a numerical and computational point of view, numerical experiments performed in this work demonstrate the ability of the present method for simulating bubbly flows with interfacial mass transfer and chemical reaction, taken into account bubble collisions, avoiding numerical merging of the fluid interfaces. From a physical point of view, bubble swarm simulation in full periodic domain shows random fluctuations in bubble velocities analogous to that observed in turbulence, whereas the averaged Reynolds number tend to the steady-state. Furthermore, these random fluctuations are observed also on the bubble surfaces. Regarding the spatial averaged chemical species concentration, it achieves the steady state after an initial transient, whereas the mass transfer coefficient tends to a quasi steady-state at $t^* \sim 40$. Altogether, this model leads

to a powerful tool for simulating mass transfer in bubble swarms, including the impact of the hydrodynamics, which are relevant to understanding the mechanisms controlling mass transfer and chemical reactions in reactive systems. Extensions of these capabilities for bubbly flows with complex chemical reactions, surfactants and phase change, in the context of the conservative level-set method introduced by [4, 5, 9], will be presented in future works.

Acknowledgments

This work has been financially supported by the *Ministerio de Economía y Competitividad, Secretaría de Estado de Investigación, Desarrollo e Innovación*, Spain (ENE2015-70672-P), and by Termo Fluids S.L. Néstor Balcázar acknowledges financial support of the *Programa Torres Quevedo, Ministerio de Economía y Competitividad, Secretaría de Estado de Investigación, Desarrollo e Innovación* (PTQ-14-07186), Spain. Three-dimensional simulations were carried out using computing time awarded by PRACE 14th Call (project 2016153612) on the supercomputer MareNostrum IV based in Barcelona, Spain.

REFERENCES

- [1] Aboulhasanzadeh, B., Thomas, S., Taeibi-Rahni, M., Tryggvason, G., 2012. Multiscale computations of mass transfer from buoyant bubbles. *Chemical Engineering Science* 75, 456-467.
- [2] Alke, A., Bothe, D., Kroeger, M., Warnecke, H.-J., 2009. VOF-based simulation of conjugate mass transfer from freely moving fluid particles. In Mammoli, AA and Brebbia, CA (Ed): *Computational methods in multiphase flow V*, WIT Transactions on Engineering Sciences, 157168.
- [3] Antepará, O., Lehmkuhl, O., Borrell, R., Chiva, J., Oliva, A., 2015. Parallel adaptive mesh refinement for large-eddy simulations of turbulent flows. *Computers and Fluids* 110, 48-61.
- [4] Balcázar, N., Jofre, L., Lehmkuhl, O., Castro, J., Rigola, J., 2014. A finite-volume/level-set method for simulating two-phase flows on unstructured grids. *International Journal of Multiphase Flow* 64, 55-72
- [5] Balcázar, N., Lehmkuhl, O., Rigola, J., Oliva, A., 2015. A multiple marker level-set method for simulation of deformable fluid particles. *International Journal of Multiphase Flow* 74, 125-142
- [6] Balcázar, N., Lemhkuhl, O., Jofre, L., Oliva, A., 2015. Level-set simulations of buoyancy-driven motion of single and multiple bubbles. *International Journal of Heat and Fluid Flow* 56, 91-107

- [7] Balcázar, N., Lehmkuhl, O., Jofre, L., Rigola, J., Oliva, A., 2016. A coupled volume-of-fluid/level-set method for simulation of two-phase flows on unstructured meshes. *Computers and Fluids* 124, 12-29.
- [8] Balcázar, N., Rigola, J., Castro, J., Oliva, A., 2016. A level-set model for thermocapillary motion of deformable fluid particles. *International Journal of Heat and Fluid Flow* 62, Part B, 324-343.
- [9] Balcázar, N., Castro, J., Rigola, J., Oliva, A., 2017. DNS of the wall effect on the motion of bubble swarms. *Procedia Computer Science* 108, 2008-2017.
- [10] Balcázar, N., Castro, J., Chiva, J., Oliva, A., 2018. DNS of Falling Droplets in a Vertical Channel. *International Journal of Computational Methods and Experimental Measurements*, Volume 6 (2018), Issue 2., 398-410.
- [11] Balcázar N., Lehmkuhl O., Castro J., Oliva A., 2018. DNS of the Rising Motion of a Swarm of Bubbles in a Confined Vertical Channel. In: Grigoriadis D., Geurts B., Kuerten H., Frhlich J., Armenio V. (eds) *Direct and Large-Eddy Simulation X. ERCOFTAC Series*, vol 24. Springer, Cham.
- [12] Gutiérrez, E., Balcázar, N., Bartrons, E., Rigola, J., 2017. Numerical study of Taylor bubbles rising in a stagnant liquid using a level-set/moving-mesh method. *Chemical Engineering Science* 164. 102-117.
- [13] Bothe, D., Koebe, M., Wielage, K., Warnecke, H.J., 2003. VOF simulations of mass transfer from single bubbles and bubble chains rising in the aqueous solutions, In *Proceedings of FEDSM03: Fourth ASME-JSME Joint Fluids Engineering Conference*, Honolulu, HI, USA, July 611.
- [14] D. Bothe and M. Kröger and H.-J. Warnecke., 2009. A VOF-Based Conservative Method for the Simulation of Reactive Mass Transfer from Rising Bubbles, *Fluid Dynamics & Materials Processing* 3, 303-316.
- [15] Bothe, D., Fleckenstein, S., 2013. Modeling and VOF-based numerical simulation of mass transfer processes at fluidic particles. *Chem. Eng. Science* 101, 283-302.
- [16] Brackbill, J.U., Kothe, D.B., Zemach, C., 1992. A Continuum Method for Modeling Surface Tension, *J. Comput. Phys.* 100, 335-354.
- [17] Clift, R., Grace, J.R., Weber, M.E., *Bubbles, Drops and Particles*. Academic Press, New York, 1978.
- [18] Chorin, A.J., Numerical solution of the Navier-Stokes equations. 1968. *Math. Comput.* 22, 745-762.
- [19] Darmana, D., Deen, N. G., Kuipers, J. A. M., 2006. Detailed 3D modeling of mass transfer processes in two-phase flows with dynamic interfaces, *Chemical Engineering & Technology* 29(9), 1027-1033.

- [20] Davidson, M.R., Rudman, M., 2002. Volume-of-fluid calculation of heat or mass transfer across deforming interfaces in two-fluid flow. *Numerical Heat Transfer, Part B: Fundamentals* 41, 291-308.
- [21] Dabiri, S., Tryggvason, G., 2015. Heat transfer in turbulent bubbly flow in vertical channels. *Chem. Eng. Sci.* 122, 106113.
- [22] Gottlieb, S., Shu, C.W., 1998. Total Variation Diminishing Runge-Kutta Schemes, *Mathematics of Computations* 67, 73-85.
- [23] Hirt, C., Nichols, B., 1981. Volume of fluid (VOF) method for the dynamics of free boundary, *J. Comput. Phys.* 39, 201-225
- [24] Koynov, A., Khinast, J. G., Tryggvason, G., 2005. Mass transfer and chemical reactions in bubble swarms with dynamic interfaces, *AIChE Journal* 51(10), 2786-2800.
- [25] Mao, Z.S., Li, T., Chen, J., 2001. Numerical simulation of steady and transient mass transfer to a single drop dominated by external resistance. *International Journal of Heat and Mass Transfer* 44, 1235-1247.
- [26] Mudde, R. Gravity-Driven bubbly flows, *Annu. Rev. Fluid Mech.* 37, 393-423. 2005.
- [27] Olsson, E., Kreiss, G., 2005. A conservative level set method for two phase flow, *J. Comput. Phys.* 210, 225-246.
- [28] Osher, S., Sethian, J.A., 1988. Fronts propagating with curvature-dependent speed: Algorithms based on Hamilton-Jacobi formulations, *J. Comput. Phys.* 79, 175-210.
- [29] Rhie, C.M., Chow, W.L., 1983. Numerical Study of the Turbulent Flow past an Airfoil with Trailing Edge Separation, *AIAA J.* 21, 1525-1532.
- [30] I. Roghair, M. Van Sint Annaland, J.A.M. Kuipers, 2016. An improved Front-Tracking technique for the simulation of mass transfer in dense bubbly flows. *Chem. Eng. Sci.* 152, 351-369.
- [31] Esmaeeli, A., Tryggvason, G., 1999. Direct numerical simulations of bubbly flows Part 2. Moderate Reynolds number arrays, *J. Fluid Mech.* 385, 325-358.
- [32] Sussman, M., Smereka, P., Osher, S., 1994. A Level Set Approach for Computing Solutions to Incompressible Two-Phase Flow, *J. Comput. Phys.* 144, 146-159.
- [33] Termo Fluids S.L., web page: <http://www.termofluids.com/>
- [34] Tryggvason, G., Bunner, B., Esmaeeli, A., Juric, D., Al-Rawahi, N., Tauber, W., Han, J., Nas, S., Jan, Y-J., 2001. A Front-Tracking Method for the Computations of Multiphase Flow, *J. Comput. Phys.* 169, 708-759.
- [35] Yang, C., Mao, Z.S., 2005. Numerical simulation of interphase mass transfer with the level set approach. *Chemical Engineering Science* 60, 2643-2660.